This manuscript is published in: Nature 500, 558-562 (29 August 2013) doi:10.1038/nature12448

Late Miocene threshold response of marine algae to carbon dioxide limitation

Clara T. Bolton and Heather M. Stoll

Geology Department, University of Oviedo, Jesus Arias de Velasco S/N, 33005, Oviedo, Asturias, Spain

Coccolithophores are marine algae that use carbon for calcification and photosynthesis. The long term adaptation of these and other marine algae to decreasing carbon dioxide levels during the Cenozoic era[1] has resulted in modern algae capable of actively enhancing carbon dioxide at the site of photosynthesis. This enhancement occurs through the transport of dissolved bicarbonate (HCO_3^-) and with the help of enzymes whose expression can be modulated by variable aqueous carbon dioxide concentration, [CO_2], in laboratory cultures[2,3]. Coccolithophores preserve the geological history of this adaptation because the stable carbon and oxygen isotopic compositions of their calcite plates (coccoliths), which are preserved in the fossil record, are sensitive to active carbon uptake and transport by the cell. Here we use a model of cellular carbon fluxes and show that at low [CO_2], the increased demand for HCO_3^- at the site of photosynthesis results in a diminished allocation of HCO_3^- to calcification, which is most pronounced in larger cells. This results in a large divergence between the carbon isotopic compositions of small versus large coccoliths only at low [CO_2]. Our evaluation of the oxygen and carbon isotope record of size-separated fossil coccoliths reveals that this isotopic divergence first arose during the late Miocene to the earliest Pliocene epoch (about 7-5 million years ago). We interpret this to be a threshold

response of the cells' carbon acquisition strategies to decreasing [CO_2]. The documented coccolithophore response is synchronous with a global shift in terrestrial vegetation distribution between 8 and 5 Myr ago, which has been interpreted by some studies as a floral response to decreasing partial pressures of carbon dioxide (pCO_2) in the atmosphere[4-6]. We infer a global decrease in carbon dioxide levels for this time interval that has not yet been identified in the sparse pCO_2 proxy record[7] but that is synchronous with global cooling and progressive glaciations[8,9].

Coccolithophores are unique among algae in that they use carbon both for calcification and for photosynthesis. Cultures of coccolithophores grown under ambient, CO_2-limiting conditions show an unusually large array (up to 5 ‰) of non-equilibrium carbon and oxygen stable isotopic fractionations ($\delta^{13}C$ and $\delta^{18}O$)[10,11]. These isotope 'vital effects', so-called because they are thought to result from biological processes, are also evident in coccoliths from recent sediments and sediment traps. The isotopic difference between small and large coccoliths diminishes in cultures grown at elevated [CO_2] (increased dissolved inorganic carbon concentration at constant pH)[12] (Fig. 1b) and is absent in fossil coccoliths from past Palaeocene greenhouse climates[13,14]. We assert that vital effects reflect the adaptation of cellular carbon fluxes to aqueous CO_2 availability, and in a new model we reveal the origin of carbon isotope vital effects. We then evaluate the timing of the emergence of vital effects in the fossil record and its relationship to Cenozoic climate evolution and the long-term decrease in pCO_2.

Photosynthesis in large cells may be more sensitive to limitation by diffusive CO_2 supply because of the lower ratio of surface area to volume (Supplementary Fig. 2).

Active transport of HCO_3^- for photosynthesis is expected to be driven by the extent of diffusive CO_2 limitation, and may therefore differ between small and large cells. A new model (Supplementary Discussion) reveals the active HCO_3^- fluxes to the cell, the site of photosynthesis (chloroplast) and the site of calcification (coccolith vesicle, CV) required to explain the observed array of carbon isotopic fractionation into organic matter and coccolith calcite, ε_p and $\varepsilon_{coccolith}$ respectively, observed in coccolithophore species of different sizes grown in culture at variable $[CO_2]$[12,15] (Fig. 1). The model confirms that at low $[CO_2]$, active HCO_3^- transport to the chloroplast is increased at the expense of active HCO_3^- transport to the coccolith vesicle. A similar competitive reallocation of HCO_3^- to photosynthesis from calcification at low $[CO_2]$ has been shown in the laboratory[16]. As a consequence, at low $[CO_2]$, a smaller proportion of calcification is supported by a direct influx of HCO_3^- to the coccolith vesicle, decreasing $\varepsilon_{coccolith}$. This process is amplified in larger cells, which at low $[CO_2]$ feature the lowest proportion of calcification supported by direct influx of HCO_3^- to the coccolith vesicle. Consequently, the difference in $\varepsilon_{coccolith}$ between large and small coccolithophores is greater at low $[CO_2]$. Culture data and our model indicate that this relationship is non-linear, with the steepest dependence of $\varepsilon_{coccolith}$ on $[CO_2]$ over the range 12-19 µM (Fig. 1b). Vital effects in $\delta^{18}O$ have previously been ascribed to changes in the relative contribution of carbonate (CO_3^{2-}) and HCO_3^- to coccolith calcite[17], which produces an effect analogous to that generated by variable relative influx of CO_2 and HCO_3^- to the coccolith vesicle predicted by our $\delta^{13}C$ model (Supplementary Discussion).

Evaluation of $\delta^{18}O$ and $\delta^{13}C$ in size-separated coccoliths from five (Integrated) Ocean Drilling Program sites (Supplementary Methods and Supplementary Fig. 9) shows that vital effects of stable isotopes in coccoliths were minimal before and after the Eocene-

Oligocene (about 34 Myr ago) and Oligocene-Miocene (about 23 Myr ago) transitions, and that large (more than 1‰) vital effects first appeared during the late Miocene to earliest Pliocene (about 7-5 Myr ago). A striking divergence in isotopic composition in different-sized coccoliths is demonstrated in records from two widely separated sites, Caribbean Site 999 and sub-Antarctic Site 1088 (Figs 2 and 3). In samples pre-dating 7 Myr ago, only small $\delta^{18}O$ and $\delta^{13}C$ differences (less than 0.75‰) between size fractions are observed. After the divergence, which begins at 6-7 Myr ago at Site 999 and 4-5 Myr ago at Site 1088, persistent vital effects of 1.5-3‰ in $\delta^{18}O$ and $\delta^{13}C$ are recorded, with large coccoliths consistently recording lighter $\delta^{18}O$ and $\delta^{13}C$ relative to smaller coccoliths (Fig. 2). We interpret this diachrony as a real lag that is too large to result from age model discrepancies (Supplementary Methods and Supplementary Fig. 11). We note that temporal changes in mean coccolith size in the sediments do not affect our data from restricted coccolith size classes.

The marked increase in vital effects in coccoliths in the late Miocene cannot reflect an expansion into a wider range of depth habitats, because the $\delta^{18}O$ and $\delta^{13}C$ values in different-sized coccoliths are positively correlated (Fig. 2, Supplementary Fig. 10), not negatively correlated as would be expected from depth segregation in the photic zone[13]. We also find no cause to suggest that the depth habitat of all coccolithophores at both sites migrated from deeper CO_2-enriched to shallower CO_2-depleted waters within the photic zone (Supplementary Discussion). At Site 999, it is possible that circulation changes associated with the gradual closure of the Central American Seaway about 14 to 3 Myr ago (ref. 18) stemmed the eastward flow of CO_2-rich upwelled water from the equatorial Pacific; however, the emergence of the Panama Isthmus is not modelled to strongly affect circulation near Site 1088 (ref. 19). The shift to a large array of vital

effects in coccoliths occurs at a time when there is no evidence for large changes in coccolithophore growth rate at either site, as indicated by coccolith Sr/Ca records (Supplementary Methods and Supplementary Fig. 5). A shift from predominantly (more than 70%) diagenetic calcite to primary coccolith calcite would be required to homogenise a 1.5‰ isotopic difference in primary $\delta^{18}O$ to the less than 0.6‰ recorded in older sediments (Supplementary Fig. 8). This is not consistent with the moderate to good coccolith preservation throughout the Miocene-Pliocene at both sites evident in scanning electron microscope images (Supplementary Figs 6 and 7), nor with Sr/Ca values, which confirm biogenic rather than abiogenic (diagenetic) Sr partitioning throughout the Miocene-Pliocene study interval (Supplementary Discussion). The presence of vital effects at the Pliocene end of both records, and their absence at the Miocene end, is unlikely to result from differences in species contributions in a given size fraction over time. Counts of coccoliths in all size fractions from end-member samples show that, despite changes in species composition and size distribution over the 16 Myr study interval, the genera or families dominating each size fraction remain similar (Supplementary Table 3). For example, at Site 1088, smallest and largest coccolith size fractions in both Pleistocene and Miocene end-member samples are dominated (more than 70% $CaCO_3$) by small reticulofenestrid and *Coccolithus pelagicus* coccoliths respectively, yet only the Pleistocene sample records a large array (up to 3‰) of vital effects (Fig. 2).

Our model of coccolithophore carbon allocation suggests that the late Miocene emergence of vital effects represents a modification of carbon acquisition strategies of the cells as $[CO_2]$ decreased below a critical threshold (Fig. 1). We propose that a decrease in pCO_2 caused tropical waters (Site 999) to fall below this $[CO_2]$ threshold at

about 7 Myr ago. Because CO_2 is more soluble in cold waters, a continued pCO_2 decline into the early Pliocene (about 5 Myr ago) was required before a similar limiting [CO_2] was reached in the cooler sub-Antarctic waters of Site 1088 (Supplementary Fig. 12).

The emergence of large-scale vital effects in coccoliths in the late Miocene, rather than at earlier transitions such as the Eocene-Oligocene or Oligocene-Miocene, for which important step decreases in pCO_2 are estimated from proxies and inferred from climate records[20-23], is consistent with culture data[12], which suggest low sensitivity of $\varepsilon_{coccolith}$ to [CO_2] variation above 19 μM. At typical concentrations of dissolved inorganic carbon in the surface ocean (2050 μM) and estimated production temperatures for a typical mid-latitude site (20 °C; Supplementary Fig. 5), the range of maximum sensitivity (12-19μM [CO_2]) corresponds to pCO_2 in the range 575-375 parts per million by volume (p.p.m.v.). As [CO_2] decreases below 20 μM there is an exponential increase in the requirement for active HCO_3^- transport to the chloroplast (Supplementary Fig. 4). Since the late Miocene, further decreases in pCO_2, even to low values typical of the last glacial[13], have not resulted in a subsequent increase in the magnitude of size-related vital effects. One explanation could be that further decreases in [CO_2] were accompanied by a decrease in cellular calcification, thereby limiting further decreases in the supply of HCO_3^- to the coccolith vesicle relative to calcification. Decreased calcification in coccoliths of a given size over the Cenozoic could support the operation of such a mechanism[24,25].

Few pCO_2 proxy reconstructions cover the interval leading up to the divergence of vital effects in coccoliths (12-5 Myr ago). Alkenone-based records suggest low and stable pCO_2 during this interval (Fig. 3b). However, these estimates could be too low because of the nature of the applied corrections for temperature and phosphate

concentrations[22,26]. New alkenone-based pCO_2 estimates from the western tropical Atlantic covering the mid to late Miocene, although low in resolution, suggest substantially higher values (400-500 p.p.m.v.)[27]. Although uncertainties remain large, stomatal proxies indicate a pCO_2 decrease[7], consistent with inverse modelling of climate data[8] (Fig. 3b). Our data suggest that substantial surface ocean cooling over the last 15 Myr, up to 14 °C in the subtropics[28], may reflect an important global pCO_2 decrease that is poorly resolved by existing pCO_2 proxy records, rather than a decoupling of atmospheric CO_2 forcing and climate as suggested by some authors[28].

The appearance of large-scale vital effects in coccoliths between 7 and 5 Myr ago is synchronous with a global expansion in terrestrial C_4 plants (that is, those using the C_4 photosynthetic pathway; mostly tropical grasses) relative to C_3 plants (primarily trees) in low-latitudes and mid-latitudes[4-6,29](Fig. 3a). In some regions, such as the Himalayan foreland and Arabian Peninsula, it has been suggested that a shift to increasingly arid conditions was the dominant driver of the late Miocene rise in C_4 plants[29]. However, the shift to C_4 dominance has also been widely interpreted as a response to decreasing pCO_2, because at low ratios of atmospheric CO_2 to O_2 concentrations C_4 plants have a competitive advantage over C_3 plants[4-6]. The presence of a biochemical carbon-concentrating mechanism allows C_4 plants to decrease energetically costly photorespiration rates, and also to decrease stomatal conductance (a measure of the rate at which water and CO_2 can diffuse in or out of the leaf), thus decreasing water loss. Conditions that favour C_4 over C_3 plants are suggested to occur below a pCO_2 of about 500 p.p.m.v. when accompanied by high temperatures during the growing season (that is, at low latitudes), or at lower pCO_2 in cooler climates[4,5]. Thus, both terrestrial and marine photosynthesizers may be showing adaptation at a common pCO_2 threshold.

We show that the large array of isotopic fractionations in modern coccolith carbonate is indicative of the operation of strong carbon-concentrating mechanisms in coccolithophore cells, which became highly significant since the latest Miocene. We speculate that this change occurred as a threshold response to increased CO_2 limitation, beginning in the late Miocene in the tropical oceans and progressing to higher latitudes by the earliest Pliocene. This increase in the degree of active carbon uptake by coccolithophores will need to be accounted for in the application of ε_p to estimates of $[CO_2]$ (ref. 30). The relatively low $[CO_2]$ threshold suggested to have driven the late Miocene diversification of coccolithophore carbon acquisition strategies is consistent with estimates of less than 500 p.p.m.v. pCO_2 required to promote the tropical C_4-dominated ecosystems that also expanded over this interval[4-6]. We speculate that such a low pCO_2 threshold, affecting both marine and terrestrial primary producers, could be reversed within decades as a result of rapid anthropogenic CO_2 release and absorption by the ocean.

Methods summary

We adapt a model for the $\delta^{13}C$ composition of photosynthetically fixed carbon in diatoms[31] with an additional module for the coccolith vesicle, allowing us to simulate the $\delta^{13}C$ of coccolith calcite as a function of the passive and active carbon fluxes into the coccolith vesicle and cell (model ACTI-CO; see Supplementary Discussion). Coccolith size fractions were separated from bulk IODP sediment samples using site-specific and interval-specific settling and microfiltration protocols (Supplementary Methods). Coccolith $\delta^{18}O$ and $\delta^{13}C$ were measured on a Nu Perspective dual-inlet isotope ratio mass spectrometer connected to a NuCarb carbonate preparation system,

with an analytical precision of 0.06‰ for $\delta^{18}O$ and 0.05‰ for $\delta^{13}C$ (1σ), at Oviedo University. Mean reproducibility, based on duplicate analyses of splits of 21 random samples from Sites 999 and 1088, is 0.08‰ for $\delta^{18}O$ and 0.06‰ for $\delta^{13}C$ (1σ). Sr/Ca was determined in two coccolith size fractions at both Sites 999 and 1088. Reducing and ion-exchange treatments were first applied to clean the samples, followed by gentle dissolution in acetic acid with an ammonium acetate buffer for 12 h. Calcium content was measured on a split of all samples, which were then diluted to constant calcium concentrations for Sr/Ca analysis by inductively coupled plasma optical emission spectroscopy on a Thermo ICAP DUO 6300 at Oviedo University. Sr/Ca data were corrected for site-specific variations in sea surface temperature (Supplementary Methods). All coccolith counts were performed on standard smear slides with a light microscope under cross-polarized light at x1250 magnification. To assess preservation, coccolith samples on polycarbonate filters were mounted onto a stub, coated with gold and imaged on a JEOL 6610LV scanning electron microscope.

References

1 Tortell, P. D. Evolutionary and Ecological Perspectives on carbon acquisition in phytoplankton. *Limnology and Oceanography* **45**, 744-750 (2000).

2 Raven, J. A., Giordano, M., Beardall, J. & Maberly, S. C. Algal and aquatic plant carbon concentrating mechanisms in relation to environmental change. *Photosynthesis Research* **109** (2011).

3 Reinfelder, J. R. Carbon Concentrating Mechanisms in Eukaryotic Marine Phytoplankton. *Annual Review of Marine Science* **3**, 291-315 (2011).

4 Cerling, T. E. *et al*. Global vegetation change through the Miocene-Pliocene boundary. *Nature* **389**, 153-158 (1997).

5 Ehleringer, J. R., Cerling, T. E. & Helliker, B. R. C_4 photosynthesis, atmospheric CO_2, and climate. *Oecologia* **112**, 285-299 (1997).

6 Zhang, C. *et al*. C_4 expansion in central Inner Mongolia during the latest Miocene and early Pliocene. *Earth and Planetary Science Letters* **287**, 311-319 (2009).

7 Beerling, D. J. & Royer, D. L. Convergent Cenozoic CO_2 history. *Nature Geoscience* **4**, 418-420 (2011).

8 van de Wal, R. S., de Boer, B., Lourens, L. J., Köhler, P. & Bintanja, R. Reconstruction of a continuous high-resolution CO_2 record over the past 20 million years. *Climate of the Past* **7**, 1459-1469 (2011).

9 Zachos, J. C., Dickens, G. R. & Zeebe, R. E. An early Cenozoic perspective on greenhouse warming and carbon-cycle dynamics. *Nature* **451**, 279-283 (2008).

10 Dudley, W. C., Blackwelder, P., Brand, L. & Duplessy, J. C. Stable isotopic composition of coccoliths. *Marine Micropaleontology* **10**, 1-8 (1986).

11 Ziveri, P. *et al*. Stable isotope "vital effects" in coccolith. *Earth and Planetary Science Letters* **210**, 137-149 (2003).

12 Rickaby, R. E. M., Henderiks, J. & Young, J. N. Perturbing phytoplankton: response and isotopic fractionation with changing carbonate chemistry in two coccolithophore species. *Climate of the Past* **6**, 771–785 (2010).

13 Bolton, C. T., Stoll, H. M. & Mendez Vicente, A. Vital effects in coccolith calcite: Cenozoic climate-pCO_2 drove the diversity of carbon acquisition strategies in coccolithophores? *Paleoceanography* **27** (2012).

14 Stoll, H. M. Limited range of interspecific vital effects in coccolith stable isotopic records during the Paleocene-Eocene thermal maximum. *Paleoceanography* **20**, PA1007 (2005).

15 Rost, B., Zondervan, I. & Riebesell, U. Ligh-dependent carbon isotope fractionation in the coccolithophorid *Emiliania huxleyi*. *Limnology and Oceanography* **47**, 120-128 (2002).

16 Bach, L. T. *et al*. Dissecting the impact of CO_2 and pH on the mechanisms of photosynthesis and calcification in the coccolithophore *Emiliania huxleyi*. *New Phytologist* **199**, 121-134. doi: 10.1111/nph.12225 (2013).

17 Ziveri, P., Thoms, S., Probert, I., Geisen, M. & Langer, G. A universal carbonate ion effect on stable isotope ratios in unicellular planktonic calcifying organisms. *Biogeosciences* **9**, 1025-1032 (2012).

18 Kameo, K. & Sato, T. Biogeography of Neogene calcareous nannofossils in the Caribbean and the eastern equatorial Pacific- floral response to the emergence of the Isthmus of Panama. *Marine Micropaleontology* **39**, 201-218 (2000).

19 Schneider, B. & Schmittner, A. Simulating the impact of the Panamanian seaway closure on ocean circulation, marine productivity and nutrient cycling. *Earth and Planetary Science Letters* **246**, 367-380 (2006).

20 Kürschner, W. M., Kvacek, Z. & Dilcher, D. L. The impact of Miocene atmospheric carbon dioxide fluctuations on climate and the evolution of

terrestrial ecosystems. *Proceedings of the National Academy of Sciences USA* **105**, 449-453 (2008).

21 Pagani, M., Arthur, M. A. & Freeman, K. H. Miocene evolution of atmospheric carbon dioxide. *Paleoceanography* **14**, 273-292 (1999).

22 Pagani, M. *et al*. The role of carbon dioxide during the onset of Antarctic glaciation. *Science* **334**, 1261-1264 (2011).

23 Pearson, P. N., Foster, G. L. & Wade, B. S. Atmospheric carbon dioxide through the Eocene-Oligocene climate transition. *Nature* **461** (2009).

24 Preiss-Daimler, I., Baumann, K.-H. & Heinrich, R. Carbonate budget mass estimates for Neogene discoasters from the Equatorial Atlantic (Ceara Rise: ODP Site 927). *Journal of Micropaleontology* **31**, 169-178 (2012).

25 Stoll, H. M. *et al*. Insights on coccolith chemistry from a new ion probe method for analysis of individually picked coccoliths. *Geochemistry Geophysics Geosystems* **8**, doi:doi:10.1029/2006GC001546 (2007).

26 Pagani, M., Liu, Z., LaRiviere, J. & Ravelo, A. C. High Earth-system climate sensitivity determined from Pliocene carbon dioxide concentrations. *Nature Geoscience* **3**, 27 - 30 (2009).

27 Zhang, Y. G., Pagani, M., Liu, Z., Bohaty, S. M. & DeConto, R. A 40 million-year history of atmospheric CO_2. *Philisophical Transactions of the Royal Society A* (In press).

28 LaRiviere, J. P. *et al*. Late Miocene decoupling of oceanic warmth and atmospheric carbon dioxide forcing. *Nature* **486**, 97-100 (2012).

29 Huang, Y., Clemens, S. C., Liu, W., Wang, Y. & Prell, W. L. Large-scale hydrological change drove the late Miocene C_4 plant expansion in the Himalayan foreland and Arabian Peninsula. *Geology* **35**, 531-534, doi: 10.1130/G23666A (2007).

30 Laws, E. A., Popp, B. N., Cassar, N. & Tanimoto, J. 13C discrimination patterns in oceanic phytoplankton: likely influence of CO_2 concentrating mechanisms, and implications for palaeoreconstructions. *Functional Plant Biology* **29**, 323-333 (2002).

31 Hopkinson, B. M., Dupont, C. L., Allen, A. E. & Morel, F. M. M. Efficiency of the CO_2-concentrating mechanism of diatoms. *Proceedings of the National Academy of Sciences USA* **108**, 3830-3837 (2011).

Supplementary Information is linked to the online version of the paper at www.nature.com/nature.

Acknowledgements We thank L. Abrevaya and A. Mendez for laboratory assistance and K. Lawrence for access to unpublished data. This work used samples provided by the (Integrated) Ocean Drilling Program (IODP). The IODP is sponsored by the U.S. National Science Foundation and participating countries under management of the IODP Management International, Inc (IODP-MI). Funding for this research was provided by European Research Council grant UE-09-ERC-2009-STG-240222-PACE (H.M.S.) and a DuPont Young Professor Award to H.M.S.

Author Contributions C.T.B. and H.M.S. designed the study and wrote the paper. C.T.B. separated coccoliths and performed stable isotope, light microscope and scanning electron microscope analyses. H.M.S. designed and ran the model.

Author Information Reprints and permissions information is available at www.nature.com/reprints. The authors declare no competing financial interests. Readers are welcome to comment on the online version of this article at www.nature.com/nature. Correspondence and requests for materials should be addressed to C.T.B. (cbolton@geol.uniovi.es).

Figure captions

Figure 1: HCO_3^- allocation to the chloroplast and coccolith vesicle inferred from $\varepsilon_{coccolith}$ measured in culture. a, simplified modelled coccolithophore carbon fluxes (details in Supplementary Fig. 1). CV, coccolith vesicle, CHL, chloroplast. Dashed black arrows represent passive fluxes, and solid black arrows represent active fluxes. **b**, $\varepsilon_{coccolith}$ as a function of $[CO_2]$ (data from ref. 12; propagated analytical uncertainly 0.1‰). **c**, Coccolith vesicle HCO_3^- influx relative to calcification, **d**, Coccolith vesicle HCO_3^- influx relative to chloroplast HCO_3^- influx, **e**, Chloroplast HCO_3^- influx relative to diffusive CO_2 uptake by cell. Data in **c**-**e** are inferred from inverse model (Supplementary Information) using default parameters (Supplementary Table 1). Symbols in **b**-**e**: diamonds, *Gephyrocapsa oceanica*; squares, *Coccolithus pelagicus subsp. braarudii*. Blue shading indicates the range of steepest dependence of $\varepsilon_{coccolith}$ on $[CO_2]$.

Figure 2: Divergence of vital effects in coccoliths. a, Benthic foraminiferal $\delta^{18}O$ (ref. 9) (data points in light grey, smoothed with seven-point running mean) and $\delta^{13}C$ of smallest and largest coccoliths (coloured circles). All $\delta^{18}O$ and $\delta^{13}C$ values are measured against Vienna Pee Dee Belemnite (VPDB). See Supplementary Fig. 10 for complete size fraction data. Bubble size scales with approximate coccolith size. For the Neogene, mean values for 3-Myr time windows are shown from Sites 999 and 1088. The grey box denotes the time interval in **b**-**e** (16-0 Myr ago). **b**, **c**, $\delta^{18}O$ (**b**) and $\delta^{13}C$ (**c**) of different-sized coccoliths from Site 999. **d**, **e**, $\delta^{18}O$ (**d**) and $\delta^{13}C$ (**e**) of different-sized coccoliths from Site 1088. To remove secular trends and highlight differences between size fractions, all coccolith isotopes are normalized to the smallest coccolith size fraction in each sample. Note the different scales of $\delta^{18}O$ and $\delta^{13}C$ axes.

Figure 3: Evolution of vital effects in coccoliths, C_4 photosynthesis, and pCO_2 since 16 Myr ago. a, $\delta^{13}C$ difference between smallest and largest coccolith size fractions at Sites 999 (red) and 1088 (orange) and the range of tooth enamel $\delta^{13}C$ values (blue shading; data from ref. 4; only North American data <37° plotted; however other regions show a similar pattern). The propagated analytical uncertainty on coccolith $\delta^{13}C$ differences is 0.07‰. **b**, Estimates of pCO_2 from various proxies: foraminifer boron isotopes (blue and yellow horizontal crosses), stomata (red diagonal crosses), alkenone $\delta^{13}C$ maximum and minimum estimates (pink, green, grey and orange shading), and inverse modelling of deep-sea $\delta^{18}O$ (black line). Note the change in scale at 500 p.p.m.v. Vertical error bars represent the uncertainty reported in published pCO_2 estimates. See Supplementary Information for pCO_2 data references and details of uncertainty derivation for each reference.

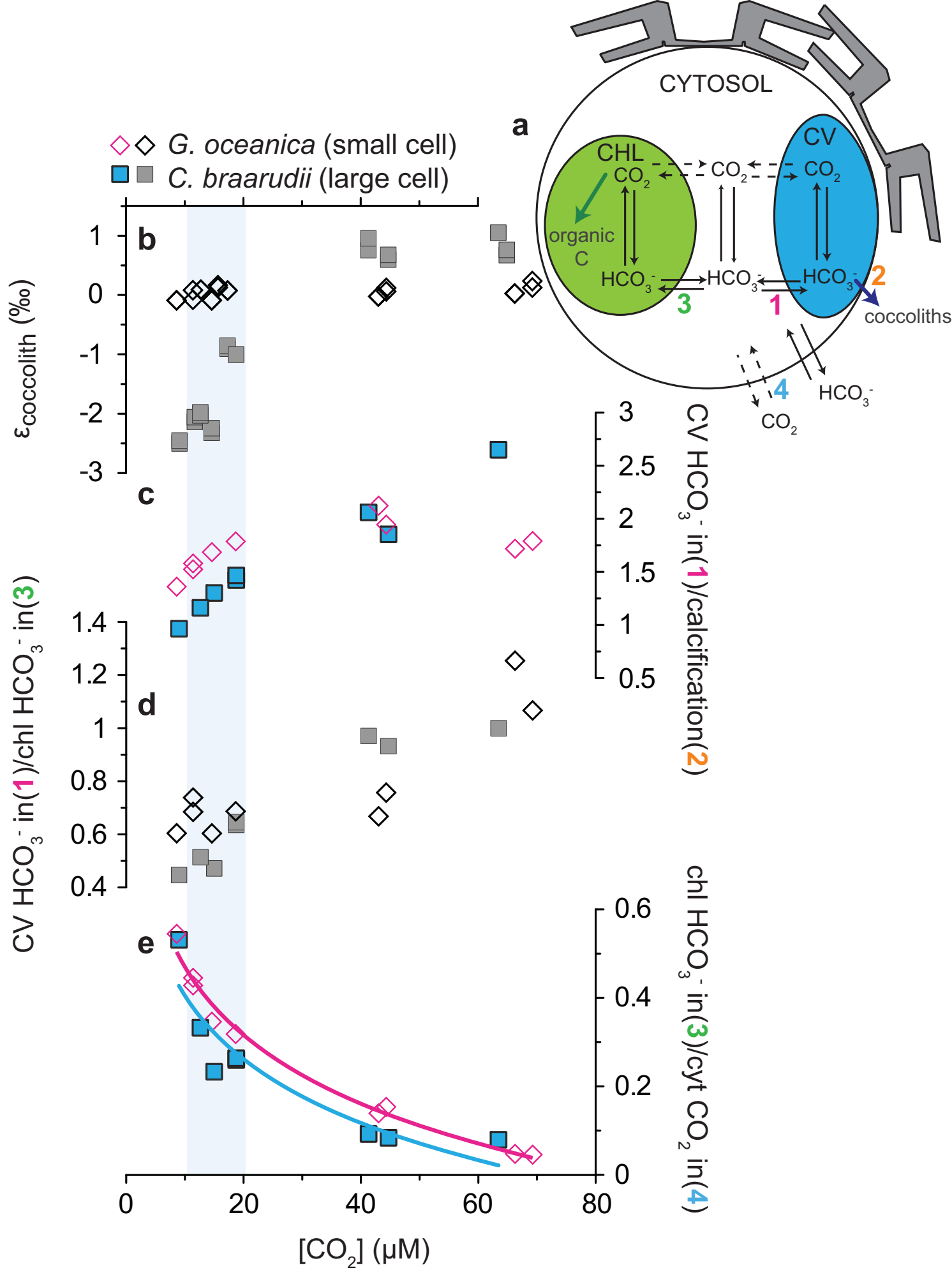
G. oceanica (small cell)
C. braarudii (large cell)
a
CYTOSOL
CHL
CV
organic C
CO2
HCO3-
1
2
3
4
coccoliths
b
c
d
e
εcoccolith (‰)
CV HCO3- in(1)/calcification(2)
CV HCO3- in(1)/chl HCO3- in(3)
chl HCO3- in(3)/cyt CO2 in(4)
[CO2] (μM)

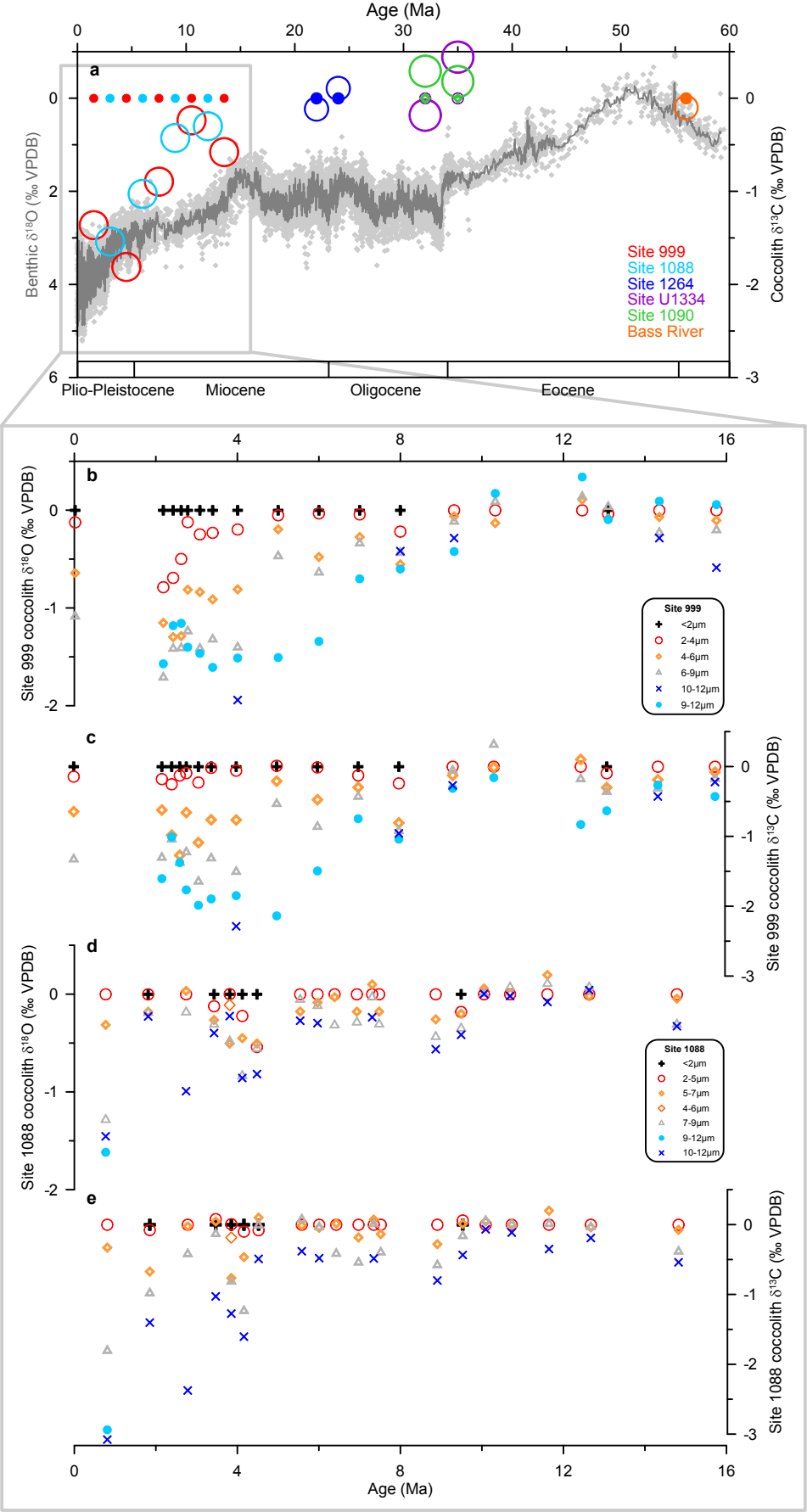
Age (Ma)
a
Benthic δ18O (‰ VPDB)
Coccolith δ13C (‰ VPDB)
Site 999
Site 1088
Site 1264
Site U1334
Site 1090
Bass River
Plio-Pleistocene
Miocene
Oligocene
Eocene
b
Site 999 coccolith δ18O (‰ VPDB)
Site 999
<2μm
2-4μm
4-6μm
6-9μm
10-12μm
9-12μm
c
Site 999 coccolith δ13C (‰ VPDB)
d
Site 1088 coccolith δ18O (‰ VPDB)
Site 1088
<2μm
2-5μm
5-7μm
4-6μm
7-9μm
9-12μm
10-12μm
e
Site 1088 coccolith δ13C (‰ VPDB)
Age (Ma)

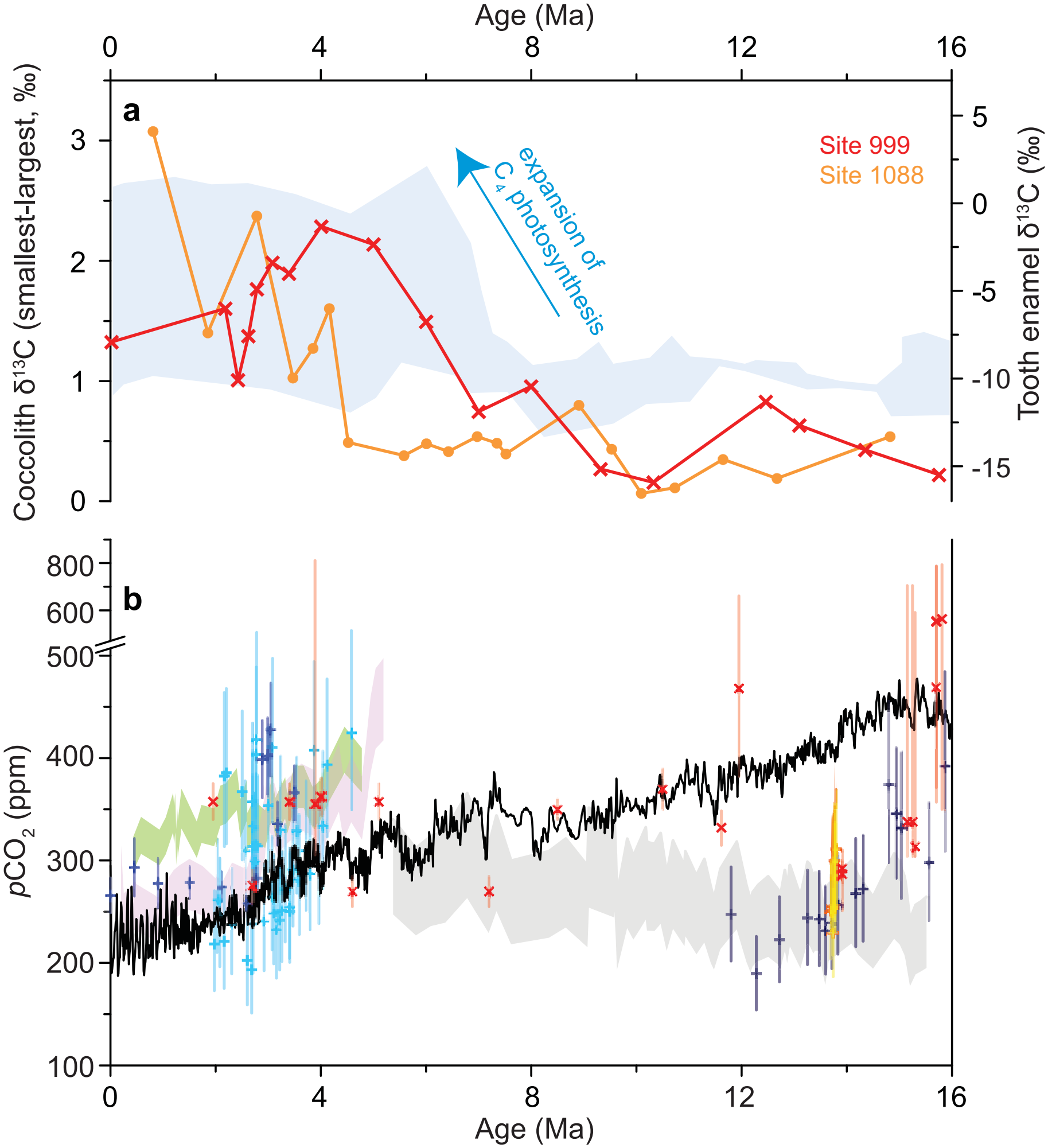
Age (Ma)
0
4
8
12
16
a
Coccolith δ13C (smallest-largest, ‰)
Tooth enamel δ13C (‰)
Site 999
Site 1088
expansion of
C4 photosynthesis
b
pCO2 (ppm)
100
200
300
400
500
600
800